Determining the potential of otolith and tissue microchemistry for the traceability of glass eels 2

An EMFF / MMO Funded project
Project number: ENG1937
Date: 30 May 2019

Authors
Florian Stein: f.stein@tu-braunschweig.de
Andreas Zitek: andreas.zitek@ffoqsi.at
Clive Trueman: trueman@noc.soton.ac.uk
David Bunt: davidbuntseg@gmail.com

Content

1. Purpose **1**
2. Background **2**
3. Objectives **2-3**
4. Methodology **3-10**
5. Results **11-22**
6. Discussion **22-25**
7. Conclusions **25**
8. Recommendations **25**
9. Acknowledgement **25**
10. References **26**

1. Purpose

This is the final report in fulfilment of the terms of the grant funding by the Marine Management Organisation and European Maritime Fisheries Fund, for project number ENG1937.

Background

2.1 Illegal trafficking in live European glass eels (juveniles) has been identified as a serious threat to the species' (*Anguilla anguilla*) survival. Europol announced in April 2018[1] that it is believed that 100 tonnes (about 300 million fish), which equates to about a quarter of the annual glass eel recruitment[2], are trafficked annually to Asia. The trafficking is enabled by a serious lack in transparency and traceability of live glass eel trade throughout the supply chain.

2.2 Traceability of eels is a requirement of the EC Eel Regulation (EC 1100/2007). Article 12 states that:

> *No later than 1 July 2009, Member States shall:*
>
> *— take the measures necessary to identify the origin and ensure the traceability of all live eels imported or exported from their territory.*

2.3 In 2009, the Convention on International Trade in Endangered Species of Wild Fauna and Flora (CITES) listed European eel in Appendix II. As a consequence, the species can be commercially traded along with CITES permits that can only be issued if it has been proven that the trade is not detrimental to the species. In 2010, the European Union concluded that they cannot ensure that trade would not be detrimental and consequently all trade of European eel (*Anguilla anguilla*) from and into the EU was suspended. The EC Eel Regulation sets a clear framework (see 2.2) and demands the identification of origin and traceability of all live traded eels.

2.4 Three major factors impede the traceability of live traded European glass eels across Europe and beyond:

2.4.1 The species range of *A. anguilla* exceeds the borders of European Union and consequently eels of different origin cannot be distinguished by genetics.

2.4.2 Illegal trade of glass eel from Europe to Asia has recently been identified as one of the potential major threats for the species' survival and is estimated to account for 50% of the declared European glass eel catches and approximately one quarter of the annual recruitment when taking into account Illegal, Unreported and Unregulated fishing (IUU).

2.4.3 Countries neighbouring the EU, have increasingly exported European eels since 2010. It is uncertain if these exports from non-EU countries originate from their territories, or if shipments include eels of EU origin.

2. Objectives

3.1 Field collection of European glass eels from major source estuaries.

3.2 Analysis of trace elements, isotopic and fatty acid compositions:

3.2.1 Analysis of strontium (Sr) isotope and trace element compositions of eel bodies, eel muscle tissues and the outer portion of eel otoliths (representing the most recent life history) and across otolith transects, recovering whole life chemical environment.

3.2.2 Determination of the isotopic composition of carbon (C), nitrogen (N), sulphur (S) and fatty acid content in eel muscle tissues reflecting recent diet.

3.2.3 Determination of the isotopic composition of carbon in essential amino acids reflecting geographic differences at the base of the food web.

3.2.4 Exploratory application of non-targeted molecular screening as tool for differentiation of eels from different origin

[1] https://www.europol.europa.eu/newsroom/news/glass-eel-traffickers-earned-more-eur-37-million-illegal-exports-to-asia
[2] http://www.illegalwildlifetrade.net/2018/07/27/europes-largest-wildlife-crime-illegal-trade-of-the-european-eel/

3.2.5 Assessment of the degree of which eels can be assigned to a likely origin based on their chemical composition using statistical tools (discriminant analyses, Bayesian inference, etc.).

3.3 Report including analytical protocols and guidelines.

3. Methodology

4.1 Sampling

Sampling of glass eels and water was carried out by collaboration partners from science and conservation, operating in the target estuaries. Based on the availability of glass eel catches, we had to change some of the sites (Spain, France). Unfortunately, glass eels from Tunisia were not provided due to unavailable catches. For compensation, we added a second river from the UK.

Country	Proposed sampling sites	Conducted sampling sites
United Kingdom	River Severn	River Severn
United Kingdom	-	River Parrett
Spain	River Minho	River Orio
France	River Loire	River Vilaine
Morocco	Sebou River	Sebou River
Tunisia	Lac Du Ghar El Melh	-

Table 1: Proposed and conducted sampling sites

River catchment	North	West	Date	Time	Water samples	Glass eel samples
Parrett UK	51.116181	-2.976935	18/04/2018	11:00 AM	3	3 x 50
Severn UK	51.882848	-2.276935	18/04/2018	04:00 PM	3	3 x 50
Orio Spain	43.282848	-2.126935	17/12/2017	04:30 AM	3	3 x 50
Vilaine France	47.498988	-2.383332	21/03/2018	03:00 PM	3	3 x 50

Table 2: Sampling details

In case of the samples from Morocco, glass eels were sampled but could not be provided to the laboratories in time. Logistic companies refused to transport the frozen samples from Morocco into the EU and communication with the institution that carried out the sampling, was extremely challenging. Emails and phone calls remained unanswered which prevented identification of alternative shipping methods in time.

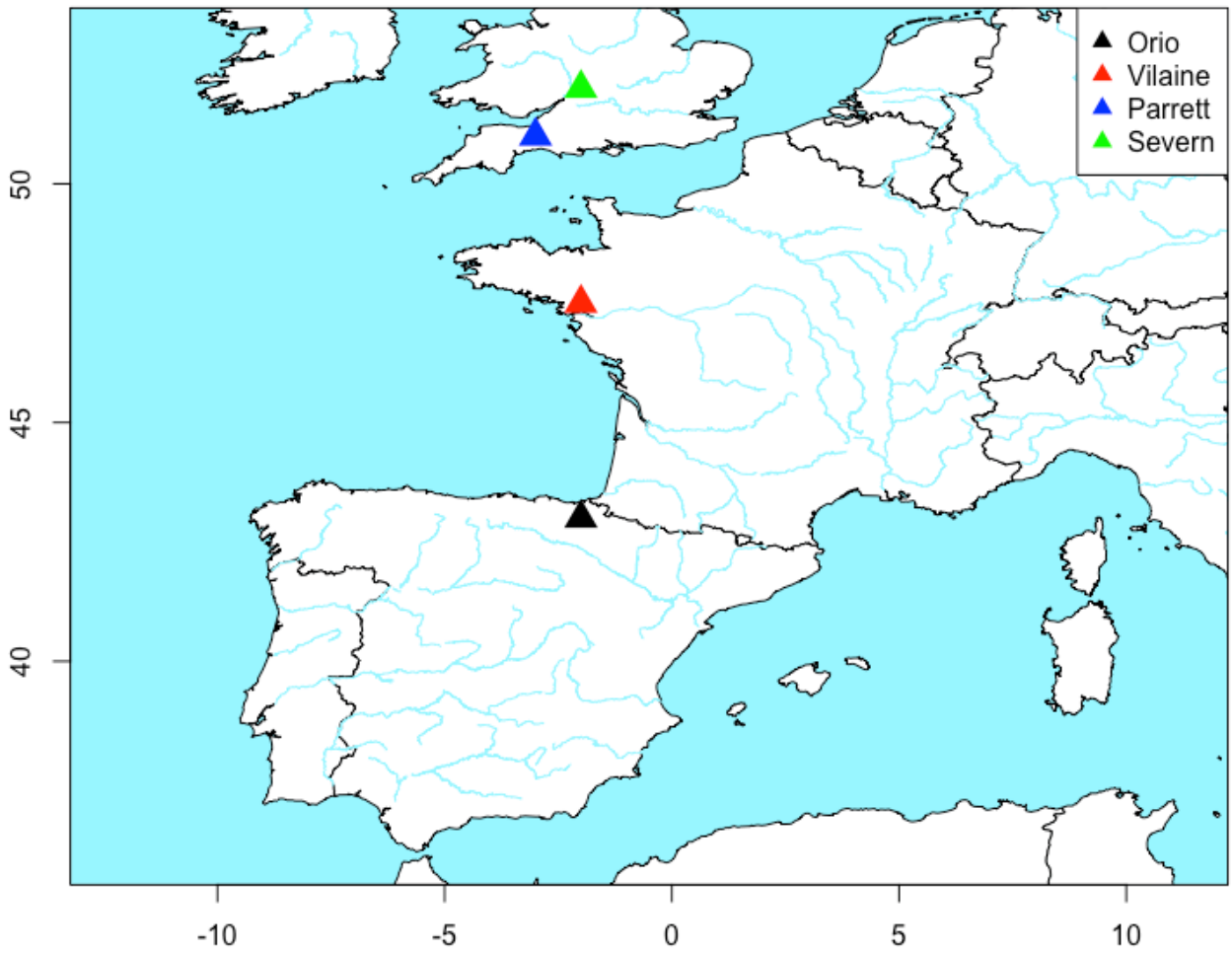

Figure 1: Map showing the samples sites across Europe

4.2 Stable isotope analyses at the University of Southampton (SOTON)

4.2.1 Sample preparation

SOTON initially co-ordinated receiving samples and initial processing of glass eels. Each sample of eels was divided and eels individually coded and transferred to separate plastic vials. The proximal (front) 1/3-1/2 of each eel was severed and sent to BOKU for trace element and Sr isotopic analyses. The remaining distal section of each eel was retained in Southampton for isotopic (and potentially fatty acid) analyses.

4.2.2 Preparation for isotopic analyses

Initial tests were performed to determine whether muscle tissue could be excised from skin and other tissues in an attempt to reduce potential complications in interpretation relating to differential contributions from tissues with differing protein or lipid compositions. The small sample size and nature of the samples made accurate and efficient sub sampling essentially impractical, and a decision was made to draw inferences from whole caudal body samples (avoiding anterior tissues such as gut, liver stomach etc).

Accordingly, anterior samples from each glass eel section were frozen and lyophilized, ground to a powder and approximately 3mg of powder weighed into tin crucibles for determination of carbon, nitrogen and sulphur stable isotopes.

4.2.3 Isotopic analyses

Analysis was performed on an Isoprime 100 isotope ratio mass spectrometer linked to a Vario ISOTOPE select elemental analyser.

Isotope data were calibrated against external standards USGS 40 and USGS41a and long-term precision monitored through analyses of an in-house amino acid standard (ACROS glutamic acid for C and N). Accuracy and precision are under 0.2‰ for each isotope. Stable isotope data are reported in delta notation as d13C, d15N and d34S values.

The lipid content of the eel tissue was estimated from carbon:nitrogen mass ratios, and a correction for the potential effect of lipid derived carbon on bulk carbon isotope data was performed according to Kiljunen et al. 2006.

4.2.4 Fatty acid analyses

Fatty acid analyses were not completed as lipid contents were relatively low (estimated at c.15-20%), requiring some optimisation of sample treatments, which had not been completed.

4.2.5 Amino acid isotope analyses

Amino acid carbon isotope analyses were not performed as initial results from the bulk carbon isotope data showed no potential for geographic differentiation among the four localities.

4.3 Analysis at University of Natural Resources and Life Sciences (BOKU)

BOKU received the individually coded proximal (front) of the glass eels and water samples and analysed otoliths and bodies by means of inductive coupled plasma sector field mass spectrometer (LA)-ICP-SFMS and a double focusing sector field in combination with a laser ablation systems (LA)-MC ICP-MS for elemental and Strontium isotope ratio. In addition, on a subset of eel bodies (n=5 per site) non-targeted molecular screening (metabolomics) was performed by a liquid chromatography time-of-flight mass spectrometer LC-ToF MS to determine potential significant complementary molecular indicators. Due to the very small size of the samples (otoliths) and low sample intake weights, existing protocols had to be optimised to meet the challenging sample preparation required for these samples.

4.3.1 Otolith extraction and processing

In a first step, to extract the otoliths, the frozen eel bodies (prior half) were taken out of the Eppendorf vials using metal forceps, and the eel heads were cut off behind the gills using a metal scissor and put in a Syracuse watch glass that was painted black on the outside (Image 1 and Image 2) following an approach for visual inspection and photographing otoliths described by Brigham and Jensen (1964).

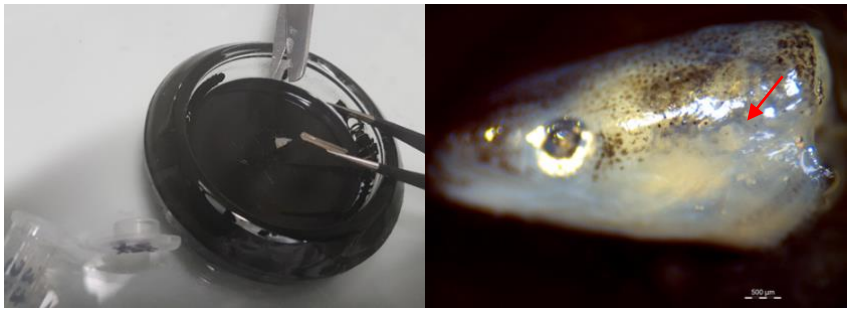

Image 1 (left) and Image 2 (right): Cutting off the head from the eel body for otolith removal behind the gills and putting it into a Syracuse watch glass painted black on the outside; the position of the sagittus otolith can be seen in Image. 2 (arrow).

Then the eel bodies were put back into the Eppendorf vial and into the refrigerator again. The head was opened from above, and brain and otoliths were removed under a binocular microscope (Image 3). The otoliths were extracted, cleaned from adhering tissue, rinsed in the water and air dried directly in the glass bowl (Image 4, Image 5 and Image 6).

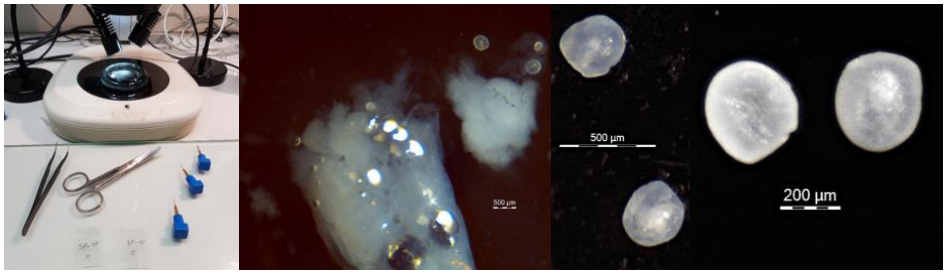

Image 3 (left) and Image 4 (mid left): Instruments used to remove the otoliths (left) and otoliths removed from eel heads (mid left). Image 5 (mid right) and Image 6 (right): Pairs of sagittal otoliths of glass eels with sulcus side up

Directly after drying for a few minutes, both sagittal otoliths per individual were affixed on cover glass strips attached to microscope slides (cut in half) sulcus side up by covering them with a drop of Krazy glue (Image 7). After 24 h of hardening, otoliths were individually ground carefully to plane using 3 µm lapping film until the core was exposed (Image 8). After grinding the material remains on the otolith sample were then removed using pressurized air. Finally, after grinding, the cover glass strip containing the rinsed otoliths was cut-off the microscope slide (Image 9) and was placed on larger glass plates (95 mm x 113 mm) for subsequent analysis (Image 10). Measurements of elements and Sr isotopes were performed on the two separate sagittal otoliths from one fish.

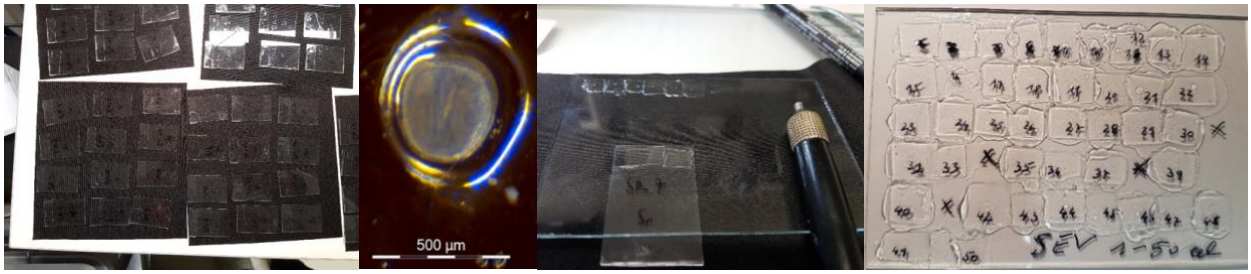

Image 7 (left): otoliths fixed to cover slide strips mounted on microscope slides with Krazy glue drying for 24 hours

Image 8 (mid left), Image 9 (mid right) and Image 10 (right): Grinded otolith and grinded otolith cut off from the cover slide strips to be mounted on larger glass slides for laser ablation.

4.3.2 Preparation of water samples, eel bodies and otoliths for digestion

Water samples were filtered, acidified with double sub-boiled HNO_3 (65%) to 4 (v/v) %. Prior to analysis, they were aliquoted, diluted 1:100 with 4% (*v/v*) sub-boiled HNO_3 (65%) and spiked with Indium as internal standard to a final concentration of 1 µg L^- respectively. Digestions of glass eel bodies was performed in a closed vessel microwave unit under cleanroom conditions. For approximately 20 - 80 mg sample intake (depending on the availability) 4 mL double sub-boiled HNO_3 (65%) and 1 mL of ultrapure H_2O_2 was used. Microwave digestion was carried out for 35 min at a power of 1400 W (maximum temperature 180 °C, maximum pressure 25 bar). The digested samples were transferred into 12 mL acid cleaned polypropylene (PP) vials, filled up to 10 g with sub-boiled water and stored at 4 °C until ICP-SFMS analysis. Certified reference materials were processed accordingly. Prior to analysis, all samples were diluted by a factor of 20 using sub-boiled water and spiked with Indium as internal standard to a final concentration of 1 µg L^{-1}.

Otoliths (n=5 per site, with some of them lost during transfer because of their small size) were digested with an open acid digestion system consisting of a programmable graphite hotplate coated with PTFE and a graphite rack for 1.5 mL PFA vials. Therefore, 1 mL of double sub-boiled HNO_3 (65%) and 200µL of ultrapure H_2O_2 was used.

Samples were digested at 105°C for 40 min on a hot-plate. Samples were evaporated and rinsed into a 12 mL acid cleaned polypropylene (PP) vial, filled up to 5 g with sub-boiled water and acidified with double sub-boiled HNO_3 (65%) to 4 (v/v) %. The certified reference materials were processed

accordingly. Prior to analysis, all samples were diluted by a factor of 20 using 4% (v/v) double sub-boiled HNO_3 (65%) and spiked with indium as internal standard to a final concentration of 1 µg L^{-1}.

4.3.3 Multi-element analysis by ICP-SFMS of water sample, eel bodies and digested otoliths

Analysis of the metals Li, B, Mg, S, Ca, Mn, Fe, Rb, Sr, Ba, Pb and U in glass eel bodies, otoliths and water samples was performed by inductively coupled plasma sector field mass spectrometry (ICP-SFMS) after respective sample preparation (see below). ICP-MS has advanced to become the most important multi-elemental atomic spectrometric routine technique for analysing trace metals in liquid samples of diverse matrix composition. As ICP-MS analysis employing quadrupole mass spectrometers is often hampered by spectral interferences and limited by the sensitivity, the present project has utilised double focusing sector field instrumentation (ICP-SFMS). Double focusing instruments permit spectral resolutions up to 10,000 and are able to separate most of the important interferences from the analyte signals. The suitability of ICP-SFMS for the determination of trace elements in complex (biological) matrices has been impressively demonstrated over the last decades. Compared to chemical resolution, the ICP-SFMS option is more straightforward, a desirable trait for analysing biological materials such as glass eel samples. For the present project, such a highly sensitive and selective ICP-SFMS was available, which has been a major pre-requisite because the concentration of some of the investigated elements was extremely low. In order to prevent sample contamination during sample processing, all analytic-chemical work has been performed in clean room laboratories of class 100.000 and 10.000 with class 100 clean benches, respectively, with temperature control (20 °C) and overpressure (+20 Pa). ICP-SFMS analysis was performed on an Element 2 under cleanroom conditions (class 10000).

Quantification of the investigated elements was carried out by external calibration (standards are prepared in diluted nitric acid) using indium as internal standard. Accordingly, ^{115}In was measured at all resolutions. Trueness of results was assessed by both, an aqueous certified reference material for controlling external calibration (TM-35 of the National Water Research Institute NWRI, Burlington, Ontario, Canada) and by solid certified reference materials as mentioned for controlling the digestion procedure. All results obtained by the described methodology are reported including their expanded uncertainty (*U*, k=2) calculated according to EURACHEM/CITAC.

4.3.4 Matrix separation for Sr isotope analysis of water samples, eel bodies and digested otoliths

Prior to Sr isotopic analysis, Sr was separated from interfering matrix elements (mainly Ca, Rb and P). Water samples and digested samples were automatically separated (Sr-matrix separation) following a standard protocol. Multi-elemental analysis and screenings were performed using an ICP-MS (NexION 350D, PerkinElmer, Waltham, MA, US) according to a standard protocol. The measurement of the $n(^{87}Sr)/n(^{86}Sr)$ ratios was performed using a multi collector ICP-MS. Separated samples were diluted with nitric acid (2% *w/w*) to obtain a mass fraction of 50 ng g^{-1}. A solution of NIST SRM 987 (NIST) was used as isotopic reference for standard sample bracketing (SSB) during Sr isotopic analysis. Concentrations of samples and SSB-standards were matched within 10%. All diluted samples and NIST SRM 987 solutions were spiked with Zr (Merck-Millipore) to allow for internal inter-elemental IIF correction.

4.3.5 Laser ablation analysis for elements

Elemental analysis was performed by coupling an NWR-213 equipped with a 2-volume-cell to an Agilent 8800 ICP-MS/MS using He as carrier gas to the ICP. The following isotopes were recorded with dwell times of 0.1 s for each isotope: ^{7}Li, ^{138}Ba, ^{24}Mg, ^{11}B, ^{57}Fe, ^{64}Zn, ^{88}Sr, ^{43}Ca, ^{55}Mn, ^{90}Zr, ^{208}Pb, ^{238}U, ^{32}S, resulting in a total of approx. 90 s analysis time for each sample. The multi-element pattern of the otoliths was measured using the operational parameters given below. One line across the entire otolith was

measured. A gas blank was measured prior to each ablation for blank correction. In-house pelleted MACS3 and FEBS1 were used as matrix-matched quality control standards.

Measurement parameters for elemental analysis
LASER: NWR-213, 213 nm solid state laser with TV2 cell (2-volume-cell)
He as carrier gas (800 mL/min)
Spot size: 30 µm
Scan speed: 2 µm/s
Laser energy: 30 %
Frequency: 10 Hz

A gas blank was measured for about 45 seconds prior to each laser ablation and an average blank value was calculated. This value was considered above the detection limit when the blank corrected value exceeded the standard deviation of the blank by three times. Subsequently element to ^{43}Ca ratios were calculated for element signals above the detection limit.

4.3.6 Data evaluation laser ablation data of otoliths – elements

Each otolith was measured by a cross sectional line scan. Before the time resolved elemental laser ablation data could be analysed, the appropriate section representing only data collected from the otolith and not being contaminated by the embedding material needed to be selected for each line. This was done by evaluating the levels of B, Zn, and Mg, which were significantly increased by the embedding material together with the increase of Ca and Sr indicating the existence of otolith material. The starting and end points of the lines were then set at the plateau of the Ca values combined with the lowest B and Zn levels. Next, the outliers were removed by a moving window approach (the mean value of 12 data points was calculated and all values out of the ± 3SD range were excluded). 12 data points reflected the spot size of 30 µm.

Finally, mean values of the Li/Ca, B/Ca, Mg/Ca, S/Ca, Mn/Ca, Fe/Ca, Zn/Ca, Sr/Ca, Zr/Ca, Ba/Ca, Pb/Ca and U/Ca were calculated across the whole otolith. To determine possible changes at the edges of the otoliths, mean values based only on data from the outer edges (30 µm on each side, 12 values per side) of each otolith were calculated. Broken otoliths and abnormal otoliths were excluded from further analysis. A stepwise linear discriminant analysis (IBM® SPSS® 24.0.0.1) was performed to identify potential discriminating variables between groups.

4.3.7 Laser ablation analysis for Sr isotopes

The strontium isotope ratios of the otoliths were measured with a combination of a double focusing sector field MC-ICP-MS instrument and a laser ablation system. Line scans were performed across the otolith cross section. Calibration for instrumental isotopic fractionation was done externally using NIST SRM 987.

A membrane desolvating system was interconnected between the laser to the MC ICP-MS prior to injection to allow the continuous introduction of 2 % HNO_3 (*w*/*w*) solution into the output of the laser ablation cell and a fast switch between laser ablation and solution-based analysis. Instrumental parameters for LA-MC ICP-MS analysis are given below.

Measurement parameters for elemental analysis
LASER: NWR-193, 193 nm excimer laser
He as carrier gas (800 mL/min)
Spot size: 50 µm (Images: additional lines: 35 µm)
Scan speed: 3 µm/s
Laser energy: 50 - 70 %
Frequency: 15 Hz

Measured m/z: 83, 84, 85, 86, 87, 88
Integration time: 0.2s

The certified reference materials used for elemental quantification and Sr isotope method evaluation were pressed pellets of MACS-3 ($CaCO_3$) and of fish otolith powder FEBS-1 respectively. About 60 seconds of the gas blank prior to the ablations were used for blank correction. The blank corrected values for ^{88}Sr, ^{87}Sr, ^{86}Sr and ^{85}Rb were used for the mass bias and rubidium correction following established protocols (Irrgeher et al., 2016). Only signals meeting the criteria of ^{88}Sr >0.3 V were considered for data analysis. In case of images, the criteria were reduced to ^{88}Sr>0.1 V.

4.3.8 Data evaluation laser ablation data of otoliths – Sr isotopes

For each otolith a mean value of the determined $^{87}Sr/^{86}Sr$ across the whole otolith line scan was calculated. In a first step, all values with a ^{88}Sr signal >0.3 V were selected. To smooth the data a moving average was applied and mean values based on 10 data points were calculated. From these mean values the overall mean values and standard deviations were calculated. To determine potential elevated signals at the edge of the otoliths, similar to the analysis of the elemental otolith data, a mean value of the outer 30 µm on both sides of the otolith (based on 10 values at each side) was calculated.

4.3.9 Exploratory non-targeted molecular screening of 5 eel bodies per site by LC-ToF MS

Sample preparation Five glass eel samples were selected from each of the four different sampling locations (France, River Vilaine; Spain, River Orio, United Kingdom, Rivers Severn and Parrett). The eel tissue samples (0.05 g) were mixed with ice-cold (4 °C) solvents (650 µL of chloroform, 390 µL of methanol and 260 µL of water), vortexed for 30 s, sonicated (60 min) and centrifuged (15min; 2200 rpm) using a GeneVac EZ 2. As the eel tissue sample weight varied from 0.02g to 0.07g, the volume of extraction solvent was normalized to the mass tissue to ensure identical ratio of tissues and solvents for all samples (as the ratio can influence the extraction recovery of metabolites). Aqueous fraction was filtered into LC glass vials using ultra-0.5 mL centrifugal filters, 100K before injection to LC-ToF MS.

Metabolomics analysis A total of 20 eel tissue samples (five replicates from each sampling location) were extracted as described above and analysed by 1290 Infinity II HPLC system coupled to a 6230 ToF MS equipped with a Dual Jetstream ESI interface.

HPLC separation was achieved using ZORBAX SB-Aq column (150 x 2.1 mm, 1.8 µm) coupled to ZORBAX SB-C8 Guard (5 mm x 2.1 mm, 1.8 µm). Mobile phase A consisted of water with 0.1% v/v formic acid, mobile phase B contained 100% methanol. Initial gradients conditions (100% A) were kept for 2 min, then increased from 0% to 40% B in the next 8 min, and was held for 2 min before starting the cleaning step. Following a cleaning step and suitable reequilibration time (5.9 min), the total analysis time was 20 min per injection. A constant flow rate of 0.250 mL/min was used, an injection volume of 5 µL, and the column temperature was 45°C.

For TOFMS detection, mass spectra between 50 and 1700 m/z were recorded in positive and negative polarity mode with following settings: drying gas temperature 120°C, drying gas flow 10 L/min, nebulizer pressure 40 psig, sheath gas temperature 350°C, sheath gas flow 12 L/min, capillary voltage 3500 V, and fragmentor voltage 120 V. The 2 GHz extended dynamic range detection mode with an acquisition rate of two TOF spectra/s was used for all measurements. The MS system was operated using both the positive-ion (ESI+) and negative-ion (ESI) modes with the mass range set at m/z 50–1700 in full scan resolution mode.

For quality control (QC), mixtures of standards (amino acids and metabolites) and mixtures of all eel samples (pool of equal volumes of each sample) were included in the injection sequence (every 7 samples). These injections were used for monitoring performance of the LC–TOF MS system. All samples were injected in a random sequence order.

Initial data processing and evaluation Various software packages associated with the LC ToFMS MS were used for data acquisition and processing. Data were acquired using Agilent Mass Hunter Data

Acquisition Workstation. Processing and analysis (peak detection, alignment and data mining) of the data was performed using MassHunter Profinder 10.0 software. Multivariate statistical analysis was performed. Prior to the PCA, the data were pre-processed using the Pareto scaling. The quality of the models was described by R2 (goodness of fit) and Q2 (predictability) values. PCA-X and OPLS-DA models were validated using 7-fold cross-validation. Cross-validation is an internal predictive validation method for determining the number of significant components by calculating the total amount of explained X-variance (R2X), Y-variance (R2Y), and cross-validated predictive ability (Q2Y).

As an additional exploratory analysis, a stepwise linear discriminant analysis (SPSS) was applied to identify potential metabolomic parameters contributing to a successful discrimination of samples.

4. Results

5.1 Data from stable isotope analysis (SOTON)

5.1.1 Tissue composition CNS data

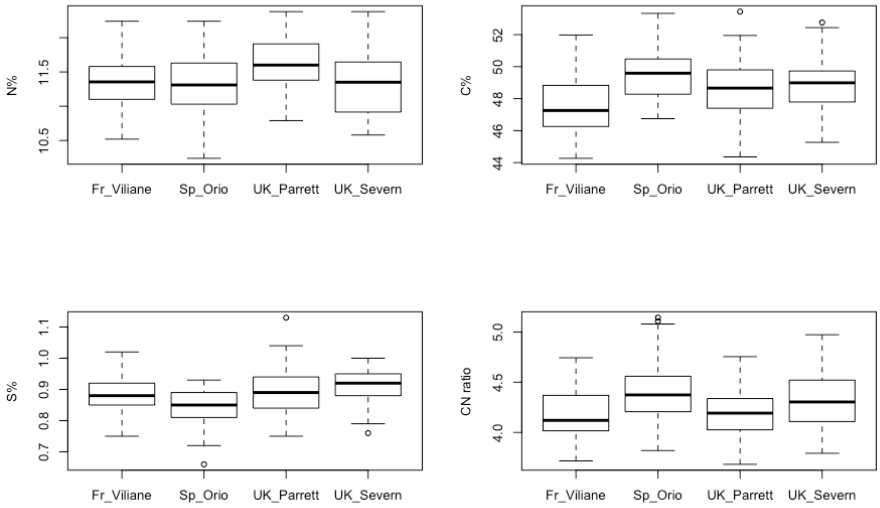

Figure 2: tissue compositions (wt % carbon, nitrogen, sulfur and CN ratio) among the four sampled locations.

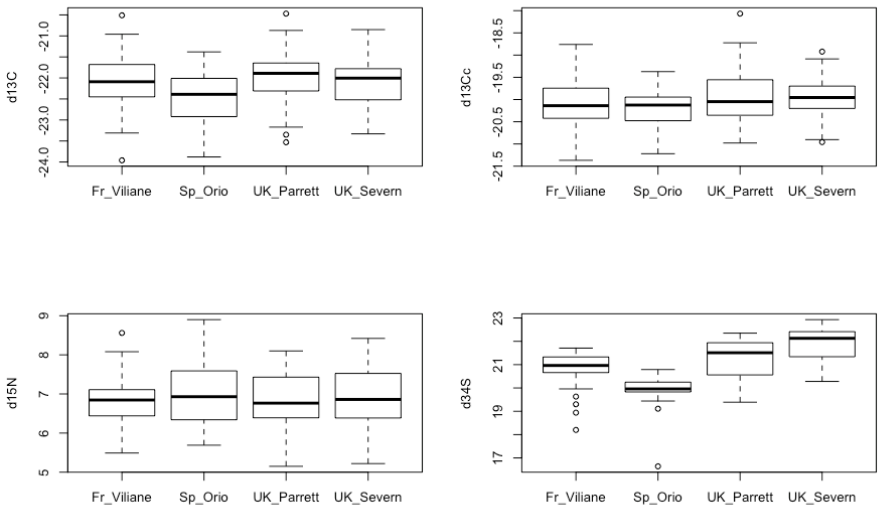

Figure 3: Stable isotope compositions among the four sampled locations. Carbon isotope data is shown as raw (d13C, A) and lipid corrected (d13Cc, B) values

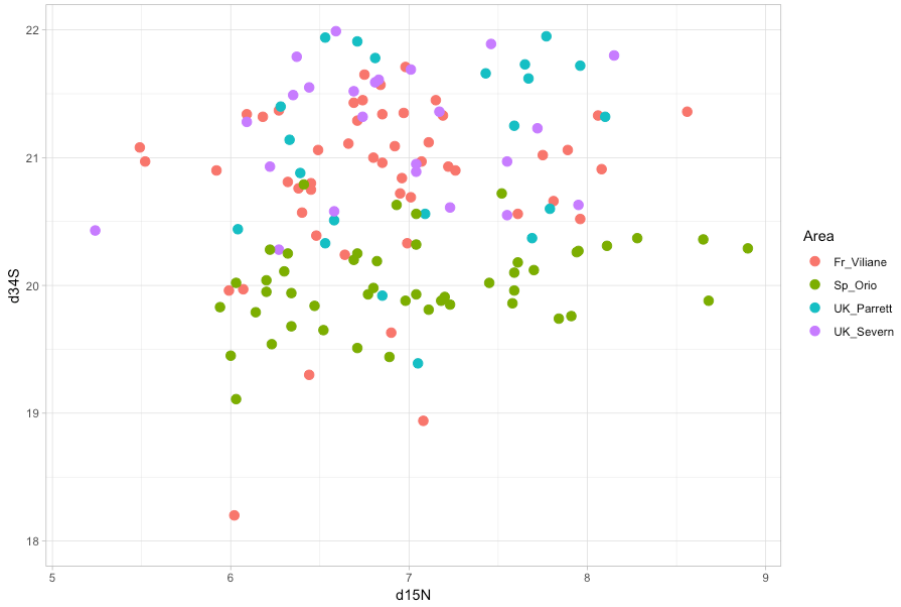

Figure 4: Stable isotope data from individual eels d34S/d15N

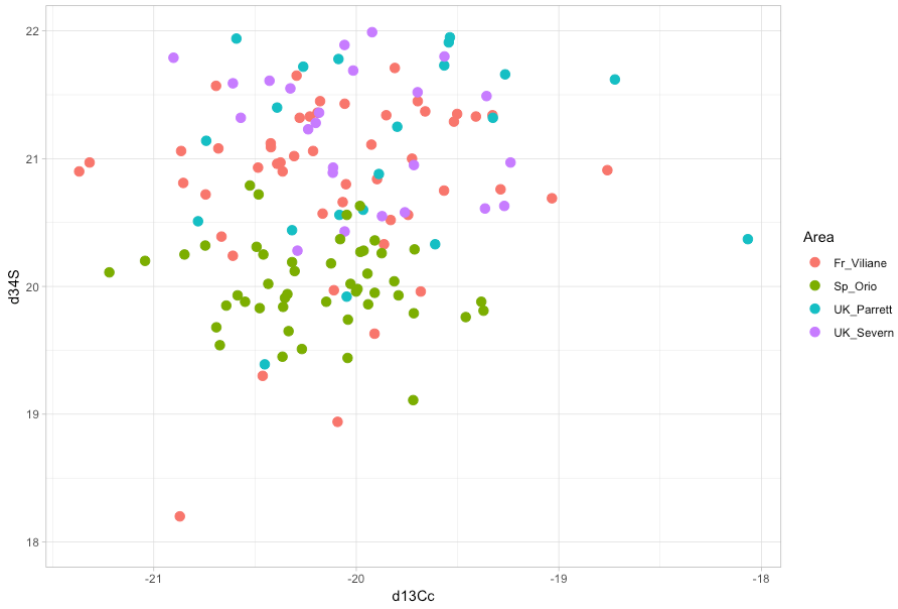

Figure 5: Stable isotope data from individual eels d34S/d13Cc

5.2 Data from multi-element analysis (BOKU)

5.2.1 Water samples

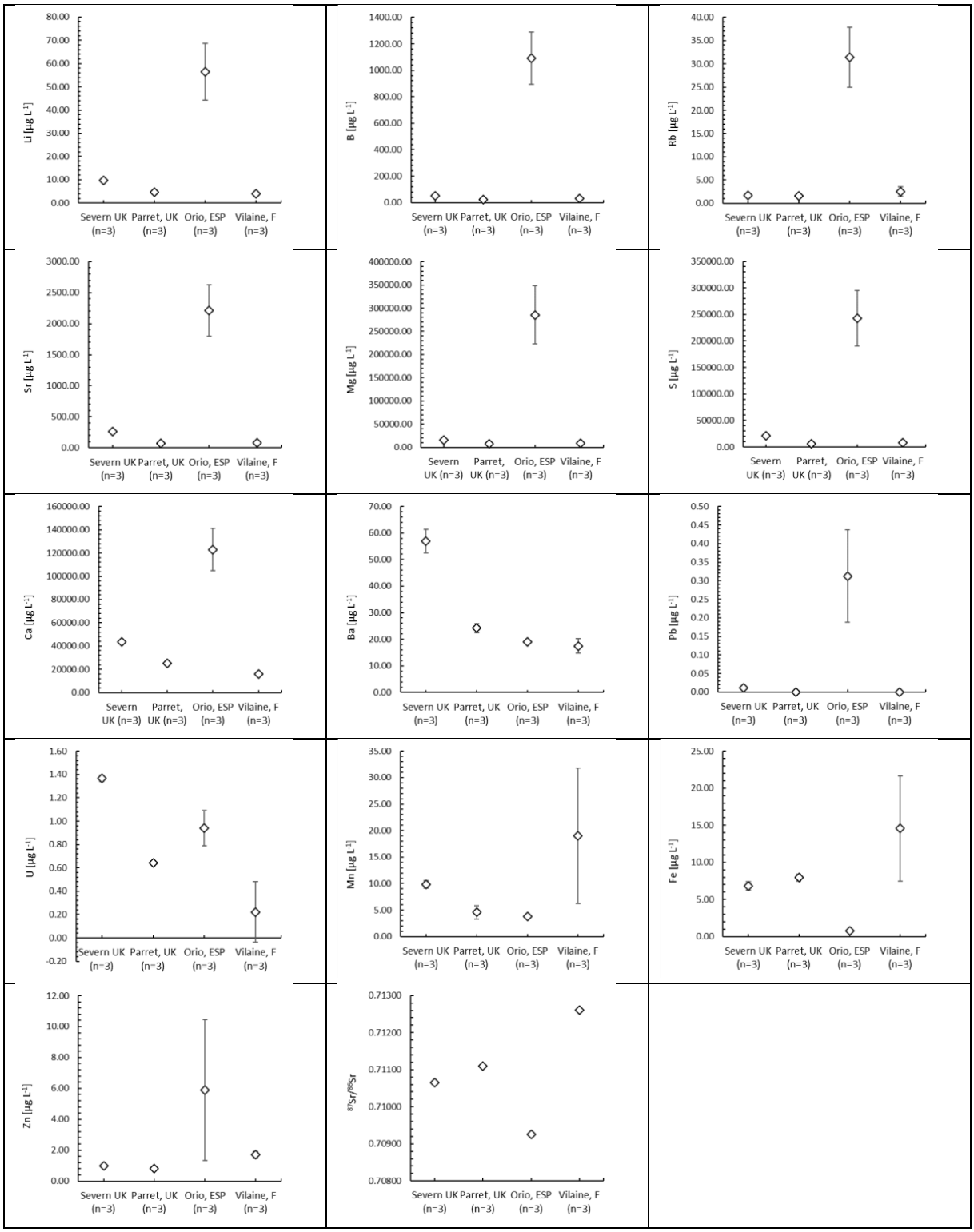

Figure 6: Elemental concentrations (µg L-1) and $^{87}Sr/^{86}Sr$ isotope ratios of four rivers (Parrett, UK; Severn, UK; Orio, ESP; Vilaine F) determined by triplicate samples per site, error bars are standard deviations based on the triplicate samples

Parameter	SEV_W_1	SEV_W_2	SEV_W_3	PAR_W_1	PAR_W_2	PAR_W_3	ORI_W_1	ORI_W_2	ORI_W_3	VIL_W_1	VIL_W_2	VIL_W_3	LOD	LOQ	U
Li	9.75	9.74	9.92	4.48	4.69	4.66	53.51	46.12	69.89	3.87	3.66	4.13	0.009	0.030	1.8%
B	52.98	53.42	53.14	22.68	23.51	23.45	1028.99	931.59	1312.27	40.37	33.13	25.24	0.225	0.751	6.2%
Rb	1.69	1.68	1.68	1.51	1.55	1.55	30.89	25.17	38.06	3.17	3.02	1.36	0.008	0.028	1.3%
Mg	14846.8	15243.0	15324.2	7916.9	8104.8	7953.6	288652.4	221964.3	346355.1	8660.1	8620.0	n.a.	0.0004	0.001	11%
S	20383.2	20970.3	20825.4	6006.5	6096.4	5886.6	245666.8	188307.5	293011.5	8420.7	8478.6	n.a.	0.001	0.003	11%
Ca	44182.1	41985.6	44201.0	23102.0	25876.6	26705.4	122161.1	105248.6	141478.1	16417.5	15335.4	n.a.	0.002	0.005	8.7%
Sr	263.74	248.89	262.00	69.14	75.67	78.60	2204.97	1806.52	2628.60	86.81	81.54	67.68	0.013	0.045	2.1%
Ba	62.00	55.26	53.47	22.38	25.73	24.58	19.87	18.30	18.76	15.95	15.80	20.65	0.039	0.130	1.0%
Pb	0.01	0.02	0.01	<LQ	<LQ	<LQ	0.24	0.24	0.46	<LQ	<LQ	<LQ	0.001	0.002	1.7%
U	1.39	1.36	1.34	0.64	0.66	0.62	1.03	0.77	1.02	0.07	0.07	0.52	0.000	0.0003	3.4%
Mn	10.62	9.69	9.23	3.13	5.51	5.02	3.47	4.14	3.94	26.17	26.59	4.23	0.011	0.037	6.1%
Fe	7.41	6.73	6.32	7.56	8.49	7.75	0.87	0.78	0.62	19.82	17.35	6.49	0.038	0.127	6.8%
Zn	0.95	0.96	1.01	0.81	<QL	<QL	3.81	2.73	11.11	1.85	1.54	<LQ	0.179	0.596	7.3%
$^{87}Sr/^{86}Sr$	0.71064	0.71066	0.71066	0.71111	0.71110	0.71109	0.70926	0.70921	0.70927	0.71259	0.71262	0.71260	-	-	0.027%

Table 3: Elemental concentrations (µg L^{-1}) in all measured water samples (replicate samples n=3 per site), limits of detection (LOD), limits of quantification (LOQ) and $^{87}Sr/^{86}Sr$ isotope ratios together with expanded uncertainty (U) in River Severn, UK (SEV), River Parrett, UK (PAR), River Orio, ESP (ORI), River Vilaine, F (VIL)

Parameter	SEV_W (n=3)			PAR_W (n=3)			ORI_W (n=3)			VIL_W (n=3)		
	Mean	SD	RSD	Mean	SD	RSD	Mean	SD	RSD	Mean	SD	RSD
Li	9.81	0.10	1.02%	4.61	0.11	2.49%	56.51	12.2	21.52%	3.88	0.23	6.0%
B	53.2	0.22	0.42%	23.2	0.46	1.98%	1090.95	197.8	18.13%	32.9	7.57	23.0%
Rb	1.68	0.01	0.43%	1.54	0.02	1.44%	31.37	6.46	20.59%	2.52	1.01	40.0%
Mg	15138.0	255.5	1.69%	7991.8	99.6	1.25%	285657.3	62249.5	21.79%	8640.0	n.a.	n.a.
S	20726.3	305.8	1.48%	5996.5	105.2	1.75%	242328.6	52431.8	21.64%	8449.6	n.a.	n.a.
Ca	43456.2	1273.6	2.93%	25228.0	1887.2	7.48%	122962.6	18128.1	14.74%	15876.5	n.a.	n.a.
Sr	258.2	8.12	3.14%	74.5	4.84	6.50%	2213.36	411.1	18.57%	78.7	9.88	12.6%
Ba	56.9	4.50	7.91%	24.2	1.70	7.02%	18.98	0.81	4.26%	17.5	2.76	15.8%
Pb	0.01	0.01	43.37%	0.00	-	-	0.31	0.12	39.81%	0.00	-	-
U	1.37	0.03	1.97%	0.64	0.02	2.70%	0.94	0.15	16.00%	0.22	0.26	117.2%
Mn	9.85	0.71	7.19%	4.56	1.26	27.56%	3.85	0.35	9.04%	19.0	12.79	67.3%
Fe	6.82	0.55	8.10%	7.93	0.49	6.21%	0.76	0.13	16.84%	14.6	7.09	48.7%
Zn	0.97	0.03	3.41%	0.81	0.00	0.00%	5.88	4.55	77.43%	1.70	0.23	13.3%
$^{87}Sr/^{86}Sr$	0.71066	0.00001	0.14%	0.71110	0.00001	0.13%	0.70925	0.00003	0.37%	0.71260	0.00001	0.15%

Table 4: Mean values of elemental concentrations (µg L^{-1}) and $^{87}Sr/^{86}Sr$ isotope ratios for all sites with standard deviation (SD) and relative standard deviation (RSD) in % in River Severn, UK (SEV), River Parrett, UK (PAR), River Orio, ESP (ORI), River Vilaine, F (VIL).

5.2.2 Discrimination of eel bodies of different origin multi-elemental fingerprints

Using a stepwise discriminant analysis (IBM® SPSS® 24.0.0.1), digested eel bodies could be discriminated by their origin with 75.8 % accuracy using the Sr/Ca, Rb/Ca, S/Ca, Mg/Ca and Sr/Ba ratios (Fig. 7, Tab. 5). When using the (corrected) $d^{13}C$ values in addition the classification could be improved to 80.1 % (Fig. 8, Tab. 6).

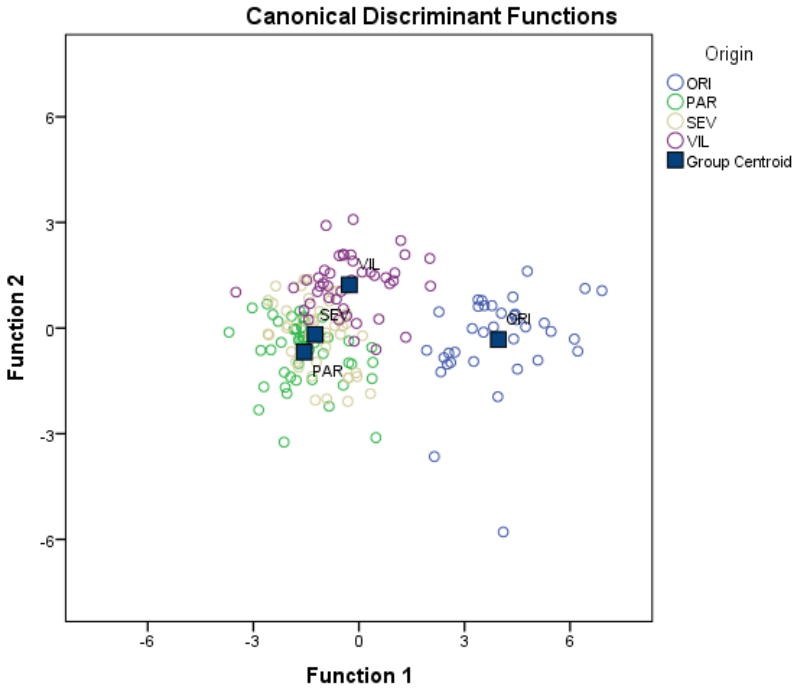

Figure 7: Discrimination of digested eel bodies according to their origin (VIL=Vilaine F; ORI=Orio ESP; PAR=Parrett UK; SEV=Severn UK) using the Sr/Ca, Rb/Ca, S/Ca, Mg/Ca and Sr/Ba ratios.

Classification Results[a]

			Predicted Group Membership				
		ggroup	ORI	PAR	SEV	VIL	Total
Original	Count	ORI	37	0	0	0	37
		PAR	0	32	17	0	49
		SEV	0	8	30	10	48
		VIL	0	1	7	36	44
	%	ORI	100,0	,0	,0	,0	100,0
		PAR	,0	65,3	34,7	,0	100,0
		SEV	,0	16,7	62,5	20,8	100,0
		VIL	,0	2,3	15,9	81,8	100,0

a. 75,8% of original grouped cases correctly classified.

Table 5: Classification result of digested eel bodies according to their origin (VIL=Vilaine F; ORI=Orio ESP; PAR=Parrett UK; SEV=Severn UK) using the Sr/Ca, Rb/Ca, S/Ca, Mg/Ca and Sr/Ba ratios.

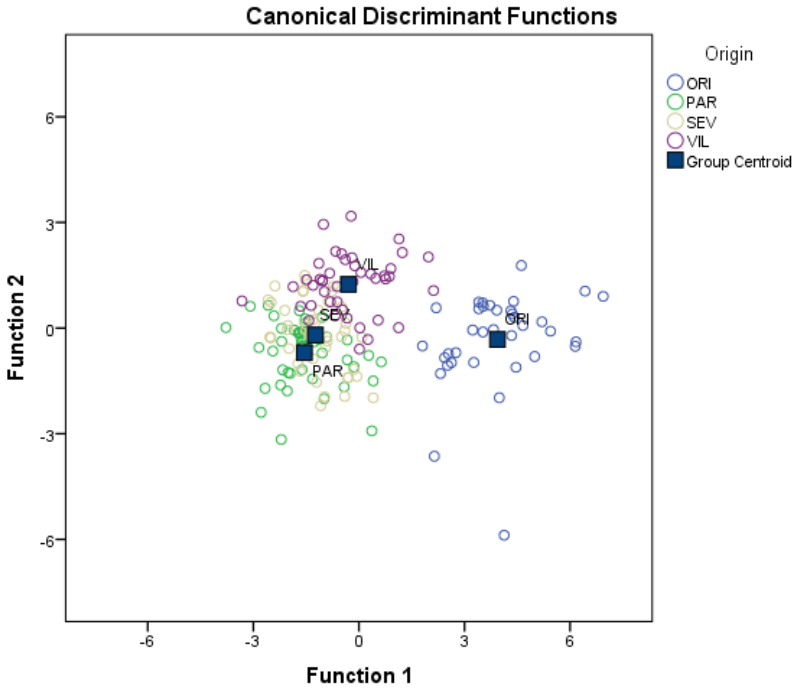

Figure 8: Discrimination of digested eel bodies according to their origin (VIL=Vilaine F; ORI=Orio ESP; PAR=Parrett UK; SEV=Severn UK) using the Sr/Ca, Rb/Ca, S/Ca, Mg/Ca, Sr/Ba ratios and d13C values.

Classification Results[a]

			Predicted Group Membership				
		ggroup	ORI	PAR	SEV	VIL	Total
Original	Count	ORI	37	0	0	0	37
		PAR	0	35	13	0	48
		SEV	0	6	33	8	47
		VIL	0	1	7	36	44
	%	ORI	100,0	,0	,0	,0	100,0
		PAR	,0	72,9	27,1	,0	100,0
		SEV	,0	12,8	70,2	17,0	100,0
		VIL	,0	2,3	15,9	81,8	100,0

a. 80,1% of original grouped cases correctly classified.

Table 5: Classification result of digested eel bodies according to their origin (VIL=Vilaine F; ORI=Orio ESP; PAR=Parrett UK; SEV=Severn UK) using the Sr/Ca, Rb/Ca, S/Ca, Mg/Ca, Sr/Ba ratios and d13C values.

5.2.3 Discrimination of eel bodies of different origin by the $^{87}Sr/^{86}Sr$ isotope ratio

The $^{87}Sr/^{86}Sr$ isotope ratios in digested eel bodies that were analysed to date (27.05.2019) were significantly different between sites (Kruskal-Wallis, p=0.000), with samples from Vilaine being highest, and differing from all other sites (Fig. 9). However, differences were within measurement uncertainties (Fig. 10).

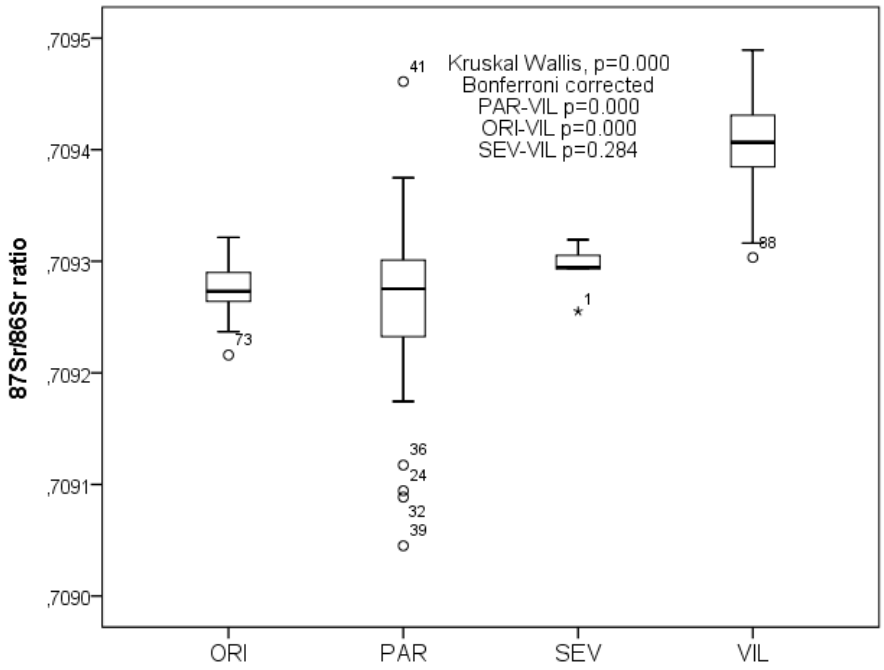

Figure 9: Differences in the $^{87}Sr/^{86}Sr$ isotope ratios in digested eel bodies from different sampling sites (VIL=Vilaine F; ORI=Orio ESP; PAR=Parrett UK; SEV=Severn UK).

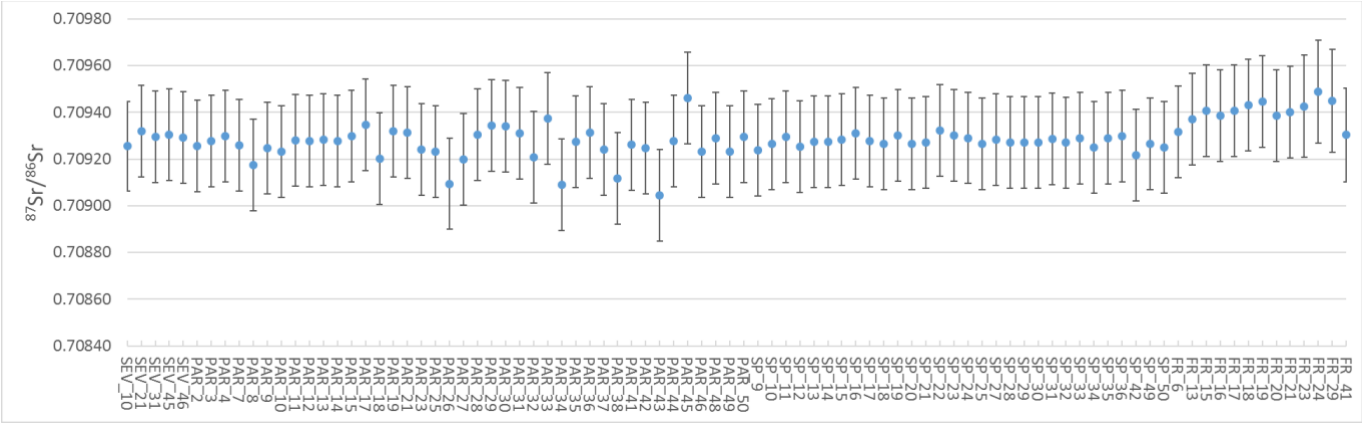

Figure 10: 87Sr/86Sr isotope ratios in digested eel bodies from different sampling sites (VIL=Vilaine F; ORI=Orio ESP; PAR=Parrett UK; SEV=Severn UK) with expanded measurement uncertainties (U, k=2).

When using the $^{87}Sr/^{86}Sr$ isotope ratios together with the Sr/Ca, Rb/Ca, S/Ca, Mg/Ca, Sr/Ba ratios for a discriminant analysis (note: only about 50 % of the Sr isotope data were available up to date), French, UK and Spanish samples could be differentiated by almost 99 % (Fig. 11, Tab. 7).

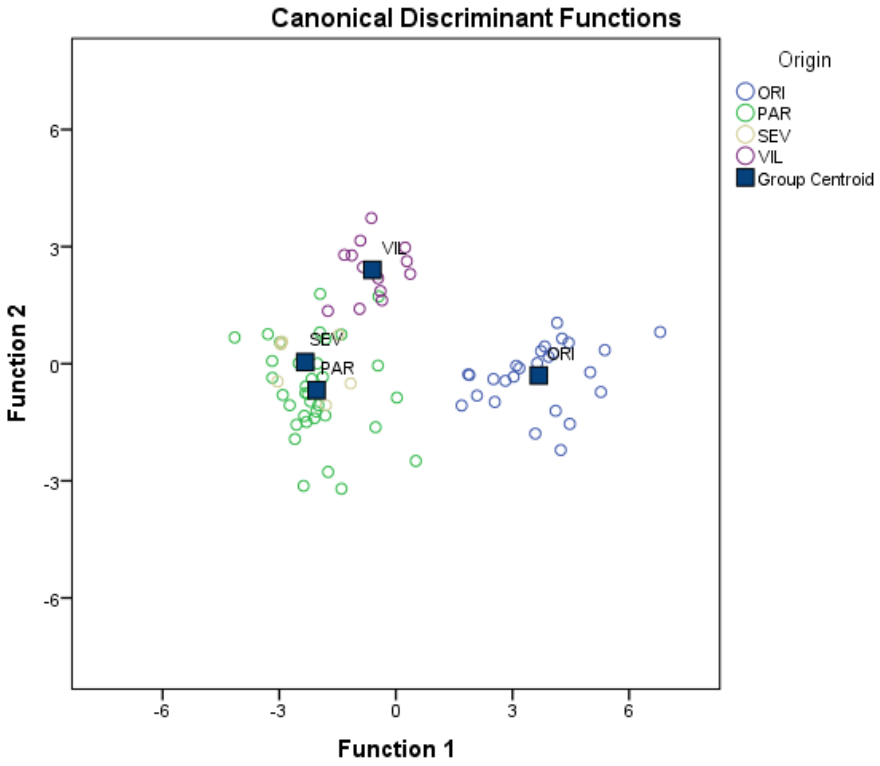

Figure 11: Discrimination of digested eel bodies according to their origin (VIL=Vilaine F; ORI=Orio ESP; PAR=Parrett UK; SEV=Severn UK) using the Sr/Ca, Rb/Ca, S/Ca, Mg/Ca, Sr/Ba ratios and $^{87}Sr/^{86}Sr$ isotope ratios.

Classification Results[a]

			Predicted Group Membership				
		gr	ORI	PAR	SEV	VIL	Total
Original	Count	ORI	26	0	0	0	26
		PAR	0	33	1	1	35
		SEV	0	4	3	0	7
		VIL	0	1	0	12	13
	%	ORI	100,0	,0	,0	,0	100,0
		PAR	,0	94,3	2,9	2,9	100,0
		SEV	,0	57,1	42,9	,0	100,0
		VIL	,0	7,7	,0	92,3	100,0

a. 91,4% of original grouped cases correctly classified.

Table 6: Classification result of digested eel bodies according to their origin (VIL=Vilaine F; ORI=Orio ESP; PAR=Parrett UK; SEV=Severn UK) using the Sr/Ca, Rb/Ca, S/Ca, Mg/Ca, Sr/Ba ratios and $^{87}Sr/^{86}Sr$ isotope ratios.

5.2.4 Discrimination of eel otoliths of different origin by element/Ca and $^{87}Sr/^{86}Sr$ isotope ratios determined by LA-ICP-MS

In total 152 otoliths could be used for the analysis (*n*=35 Vilaine F, *n*=35 Parrett UK, *n*=43, Severn UK, *n*=39, Orio ESP). The Sr/Ca ratio in the outer edge of the otoliths was identified as the only reliable and significantly differing parameter across sites (Fig. 12). Although the mean values were significantly different, discrimination of samples according to their origin was not possible by LA-ICP-MS data.

For the Sr isotope ratios (Fig. 13) no significant difference could be found for whole line scan mean values (Fig. 13) and only outer edge data.

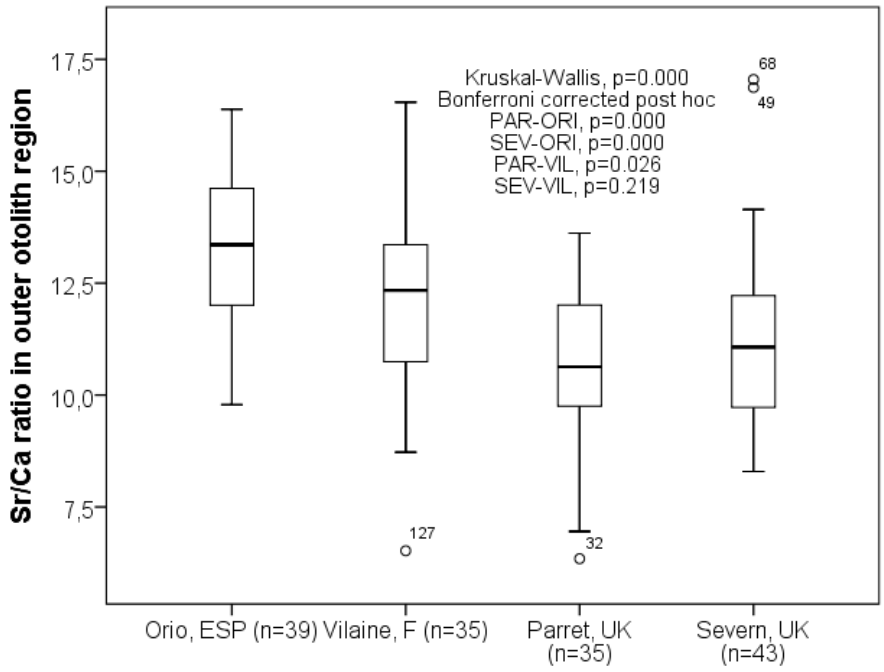

Figure 12: Differences in the Sr/Ca ratios at the outer 30 µm on both sides of the otoliths of four different sampling sites.

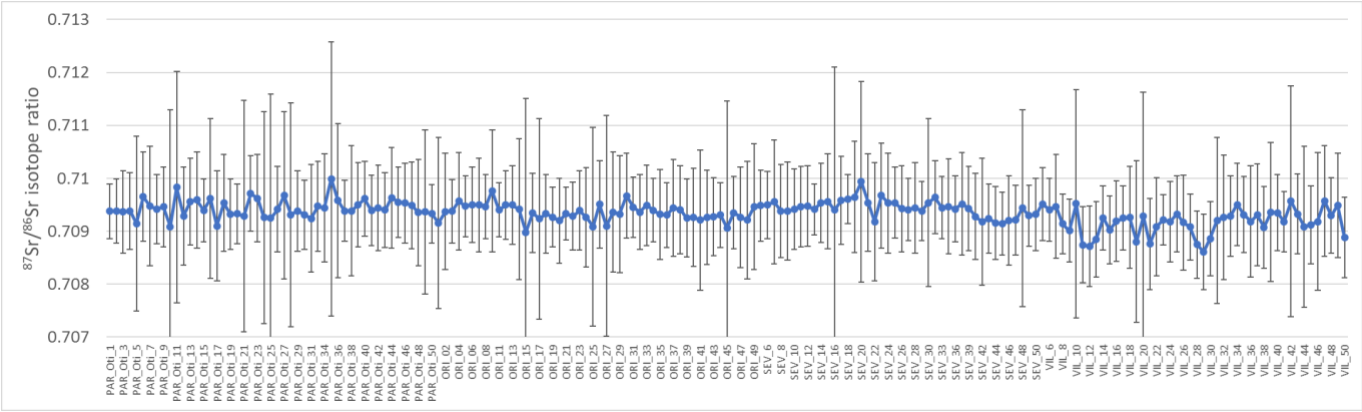

Figure 13: Mean values of $^{87}Sr/^{86}Sr$ isotope ratios across whole otoliths determined by line scans according to different sampling sites (VIL=Vilaine F; ORI=Orio ESP; PAR=Parrett UK; SEV=Severn UK); error bars are standard deviations.

5.2.5 Discrimination of digested eel otoliths of different origin by element/Ca and $^{87}Sr/^{86}Sr$ isotope ratios

Results of whole digested otoliths showed large variability with Vilaine samples showing the lowest Sr/Ca ratios (Tab. 8, Fig. 14). Due to the smallness of the otoliths two of them were lost during the transfer for digestion.

Code	Sr	Ca	S/Ca ratio
PAR_26	13.9	1355	0.0102
PAR_28	14.9	1307	0.0114
PAR_29	24.3	2061	0.0118
PAR_30	23.8	2031	0.0117
ORI_1	16.6	1321	0.0126
ORI_2	20.3	1669	0.0121
ORI_3	19.2	1835	0.0104
ORI_4	21.9	1905	0.0115
ORI_6	16.3	1499	0.0109
SEV_1	16.1	1316	0.0122
SEV_2		lost	
SEV_3	18.0	1339	0.0134
SEV_4	18.0	1295	0.0139
SEV_5	27.3	2708	0.0101
VIL_1		lost	
VIL_2	30.3	2832	0.0107
VIL_3	21.2	1990	0.0107
VIL_4	15.2	1452	0.0105
VIL_5	14.3	1347	0.0106
LOD [µg kg-1] (dil.corr)	0.22	30.9	
LOQ [µg kg-1] (dil.corr)	0.73	103	
U	15%	15%	
Recovery CRM	99%	99%	

Table 8: Sr and Ca relative concentrations (µg kg-1, not weight corrected) and Sr/Ca concentrations of digested otoliths.

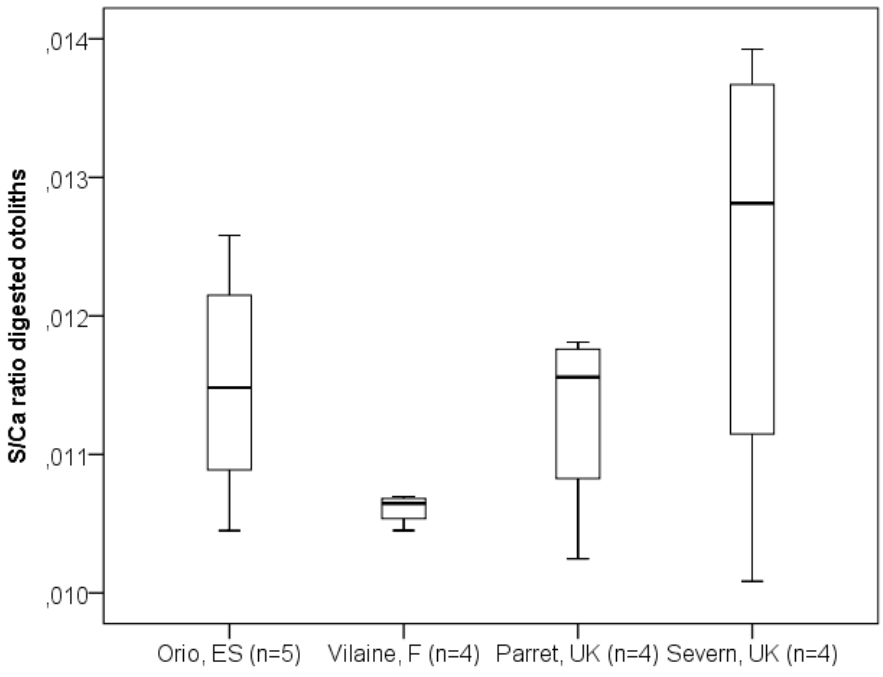

Figure 14: Sr/Ca concentrations of digested otoliths (based on µg kg-1, not weight corrected).

5.2.6 Water elemental ratios compared to the elemental ratios in eel bodies used for discrimination

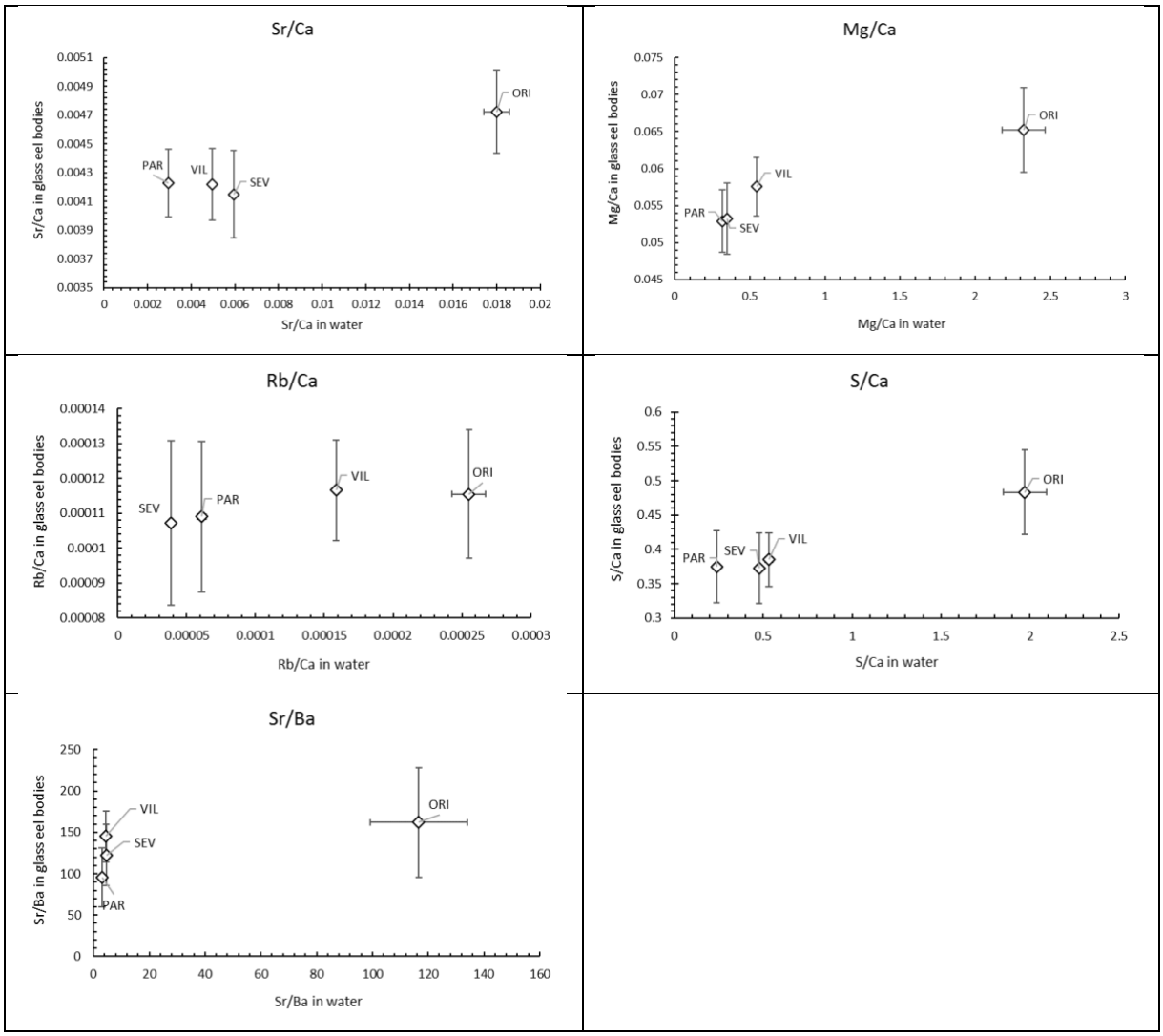

Figure 15: Water elemental ratios compared to the elemental ratios in eel bodies used for discrimination; error bars are standard deviations

5.2.7 Metabolomics

Principal component analysis (PCA) represents one of the most frequently used chemometric tools that allows projection of data from a higher to a lower dimensional space. In the preliminary investigation, PCA of metabolomics data was performed to investigate any possible clustering of glass eel samples on the basis of catchment location. As Fig. 16 shows, using PCA, there were indications of discrimination of Spanish glass eels from the rest (in both, positive and negative mode). It is apparent that more pronounced clustering and significantly better differentiation amongst sample groups was obtained for negative ionisation data (Fig. 16B) compared to those acquired in the positive mode (Fig. 16A).

The first principal component (PC1) accounted for 32.1% and 25.1% variance for positive and negative ionisation data, respectively, while second principal component (PC2) contributed to 25.2% and 17.8% for these ionization modes.

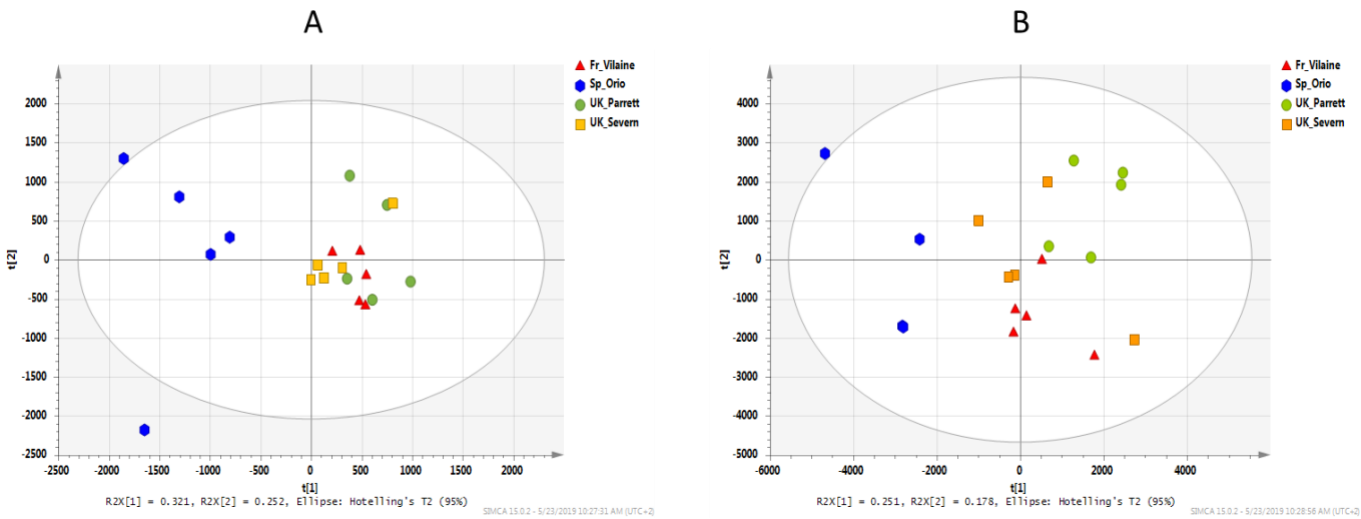

Figure 16 A/B: A/B: The PCA 2D scores plot of glass eels (from four different sampling locations France (River Vilaine), Spain (River Orio), United Kingdom (Rivers Severn and Parrett); (n = 5) metabolomics data obtained in positive (A) and negative (B) mode. The ellipse represents the 95% confidence region for Hotelling's T2

Since some clustering between glass eels of various catchment locations was observed by PCA, further supervised multivariate analysis was employed using orthogonal projection to latent structures discriminant analysis (OPLS-DA), which provides improved visualization and interpretability of the model. From the results of the OPLS-DA study, four sample groups were separated using positive mode metabolite data with a prediction rate of 67.1% (R2 = 0.794; Q2 = 0.671), while the prediction rate for metabolomic negative mode data was 72.3% (R2 = 0.832; Q2 = 0.723) (Fig. 17 A/B).

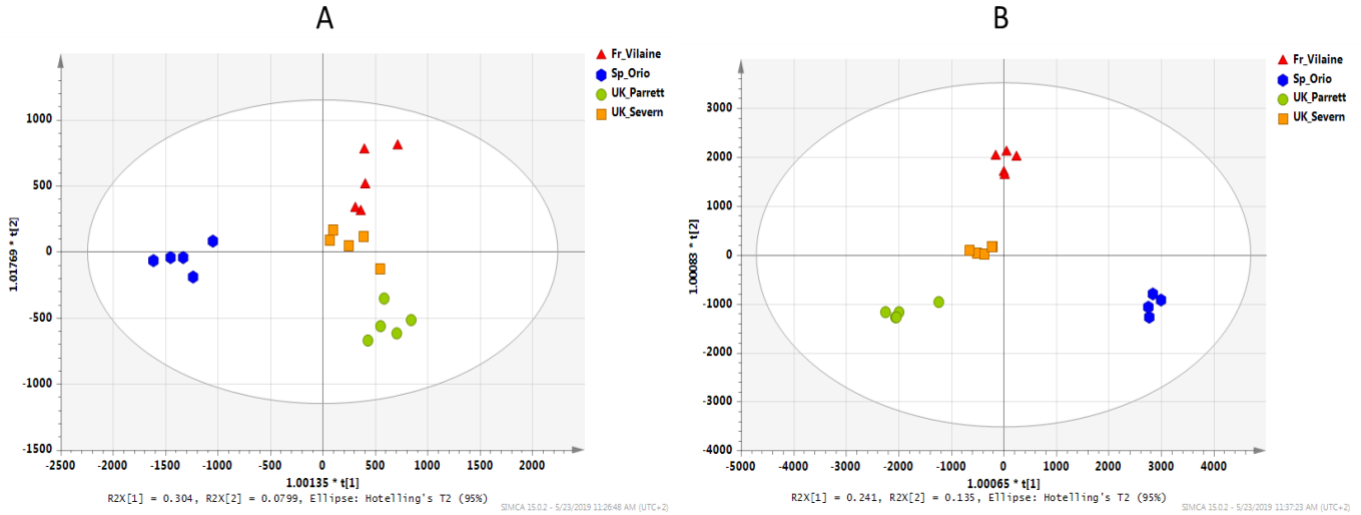

Figure 17: 17 A/B: OPLS-DA scores plots showing clustering of glass eels obtained by (A) positive and (B) negative ionization mode

When performing a stepwise discriminant analysis in SPSS, 100 % accurate classification could be achieved using only three selected variables (masses 89.0479, 88.0628 and 183.065) of positive ionisation data. In negative ionisation data, masses of 116.011, 148.038, 152.033 yielded 100 % accurate classification when combined with d13C(corrected). However, for the Parrett, in two cases the $d^{13}C$ (corrected) values were not available. In these cases, the differentiation between Severn and Vilaine seems most challenging.

5. Discussion

The character of our study is explorative as only very few studies were previously conducted to determine if eel otolith chemistry is suitable to align individual eels to locations (e.g. Evans et al 2014, Otake et al 2019). Nevertheless, studies aimed to distinguish stocked eels from natural recruited eels (Evans et al 2014) and identification of the growing habitats (Otake et al 2019) while our study aimed to explore the potential of different methodological approaches to distinguish river catchments of glass eel recruitment arrival. Due to the minimal available material from otolith zones on the edge of the tiny glass eel otoliths built during the time spent in estuaries and river habitats, the detection of the specific habitat information is the bottleneck that complicates the feasibility of otolith analysis for the planned purpose. This is why in this study the chemical composition of glass eel bodies was also analysed in addition using different approaches.

6.1.1 Stable isotope and tissue compositions

Tissue bulk element (CNS) compositions did not vary significantly among the four sampled regions. Eels from the River Orio in Spain on average had lower sulphur content and eels from the Rivers Viliane and Parrett had relatively low CN ratios, and, by inference, lower lipid contents. However, these differences were expressed at the level of population medians and were not sufficiently clear to have discriminatory power.

Tissue d13C and d15N values were remarkably consistent among the four sites, implying that muscle tissue was synthesised from a relatively consistent diet source. This could reflect either isotopically consistent diets in each estuary or, more likely, that the bulk of the muscle tissue was synthesised during growth in the open ocean prior to arrival in the distinct estuaries.

Tissue d34S values, by contrast, did differ markedly among regions, with eels from the Orio River showing consistently lower d34S values. Marine sulphate has relatively consistent d34S values, but sulphur isotopes are strongly fractionated during anaerobic microbial respiration, where sulphide oxidation releases sulphur with low d34S values. It is therefore likely that eels from the Orio River had incorporated sulphur from anoxic / wetland sediments, possibly indicating longer residence within the river influence for River Orio eels prior to sampling. Whilst this discrimination is encouraging, it is noteworthy that individual eels may show considerable variability in d34S values, with individuals from the Rivers Vilaine and Parrett displaying low d34S values implying incorporation of sulphur influenced from anoxic bottom (muddy) sediments. Again, this reinforces the issue that discriminatory power will be increased by the relative time that eels have spent in the estuarine environment relative to the rate of incorporation of elements into tissues.

Sulphur isotopes may offer more discriminatory power for two reasons – firstly the isotopic distinction between marine sulphate and microbially mediated sulphide is relatively large, and secondly skin proteins may have relatively high methionine contents compared to muscle, potentially allowing a faster incorporation of S isotopes reflecting the local estuarine environment.

The ability to discriminate among sites using just d13C and d15N values and d13C, D15N and d34S values was tested with a simple linear discriminant analyses methodology.

	Vilaine	Parrett	Severn	Orio
Vilaine	**27**	3	12	8
Parrett	7	**1**	14	4
Severn	14	0	**36**	0
Orio	6	0	0	**43**

Basic classification matrix based on a linear discriminant analysis of d13C, d15N and d34S values, using a resampling process to estimate classification accuracy. True origin displayed in rows, classified into

columns. Overall classification accuracy was 61%, with classification accuracy ranging from 88% for the River Orio to 4% for the River Parrett. Most misclassifications from the Parrett were to the adjacent River Severn, however. Combining the two UK rivers results in an improved overall classification accuracy of 70%, with 40% classification accuracy to River Vilaine, 79% accuracy to the Parrett-Severn system and 86% accuracy to the River Orio.

	UK	France	Spain
UK	**60**	13	3
France	21	**20**	9
Spain	0	7	**42**

6.1.2 Multi-element pattern and Sr-isotope pattern in eel bodies

Eel bodies showed a strong variation in elemental content and only a standardisation of the measured elemental concentrations to Ca yielded parameters that could be used to discriminate samples according to their origin. Sr/Ca, Rb/Ca, S/Ca, Mg/Ca and Sr/Ba were determined as significant parameters for discrimination using a stepwise discriminant analysis. The combination of these parameters with d13Cc (lipid corrected) slightly improved the classification result. Spanish samples could be differentiated by 100 % from all others, while French samples could be differentiated by 80 % and were mixed up by 20 % with samples from River Severn. River Parrett samples were only mixed with Severn samples. The $^{87}Sr/^{86}Sr$ isotope ratios in digested eel bodies were relatively high in samples from the River Vilaine, potentially reflecting drainage of relatively radiogenic rocks of the Amorcian massif. It is likely that Sr exchange in the body tissue of eels is relatively rapid, allowing for regional catchment-specific geochemical variations to be expressed in eels' bodies despite relatively low residence times prior to sampling.

When adding the $^{87}Sr/^{86}Sr$ isotope ratios of eel bodies to the discrimination analysis to the elemental ratios, UK, French and Spanish samples could differentiated almost by 99%.

Using just C:N ratios, d34S and $^{87}Sr/^{86}Sr$ isotope ratios as tracers, 84% of eels could be assigned correctly to country of origin, again pointing to the importance of tracers with rapid metabolic processing.

6.1.3 Elemental and Sr-isotope pattern in otoliths

Otolith strontium stable isotopic ratios ($^{87}Sr/^{86}Sr$ ratio) of freshwater fishes have been clearly shown to indicate the water characteristics of habitats occupied by the fishes. Otolith $^{87}Sr/^{86}Sr$ ratios vary in direct proportion to the ratio of ambient water, which reflects the ratio of the watershed geology, such as age and composition of rock formations (Kennedy et al. 1997, 2000, 2002; Garcez et al. 2015). Therefore, a marked geological diversity across a study area, being reflected in otolith $^{87}Sr/^{86}Sr$ ratios of fishes distributed in the area, can be expected to vary significantly among habitat tributaries. Previously inhabited tributaries of each fish can be reconstructed from the otolith $^{87}Sr/^{86}Sr$ ratio and bedrock geology (Otake et al. 2019). Nevertheless, linking determined isotopic ratios to specific bedrock geology goes beyond the study target, however the samples collected at the mouth of the rivers within this study represent an accumulated reflection of the overall catchment geology. Here, we aimed to determine if the (unknown) residence time in the different estuaries can be detected by different chemical analyses, with the analysis of otoliths by LA-ICP-MS being one of them. However, no differences in the $^{87}Sr/^{86}Sr$ isotope ratio across the whole otolith and also at the outer 30 µm of the otoliths on both sides could be detected by laser ablation although the $^{87}Sr/^{86}Sr$ isotope ratios in rivers differed significantly. The time the glass eels might have spent in the habitats influenced by the river water was obviously too short for incorporation and creation of sufficient otolith material needed for analysis.

With regard to elemental data, only the Sr/Ca ratio in the outer regions of the otoliths showed limited potential as an indicator being significantly different between some sites.

6.1.4 Metabolomics

Metabolic fingerprint analysis was shown to be an effective approach in differentiating between glass eel catchment locations (River Vilaine: France; River Orio: Spain; Rivers Severn and Parrett: United Kingdom). It is suggested that the LC–MS metabolomics approach is highly effective for biomarker identification and could thus represent a new strategy in glass eel forensics. To provide increased confidence in these results and in the applicability of the methodology, the range and number of glass eel samples needs to be expanded through additional studies.

Overall the combined data show that in order to provide geographic discrimination among glass eels sampled recently on entry into river systems, tracers must ideally be (1) rapidly introduced into the tissue under study and (2) must differ widely among sites in order to yield sufficient signal with short times available for uptake.

Biogeochemical tracers associated with more metabolically active tissues (such as metabolomics, CN ratios, body tissue Sr isotopes and elements and potentially d34S values) are likely to be more promising, but with a caveat that these tracers are inherently less predictable, more sensitive to short term environmental and behavioural fluctuations.

6. Conclusions

The project provides the following conclusions:

7.1 Sr/Ca, Rb/Ca, S/Ca, Mg/Ca and Sr/Ba $^{87}Sr/^{86}Sr$ isotope ratio in eel bodies proved to be good geographical discriminators between UK, French and Spanish samples, as they directly reflect the habitat conditions.

7.2 Otolith data could not contribute to a differentiation, as the habitat information was obviously not sufficiently incorporated in the otoliths to be detectable by LA-ICP-MS with the chosen setup.

7.3 Non-targeted molecular screening could be a valuable complementary method, when a stable relation to the geographic location can be established.

7.4 Stable isotope compositions (d13C, d15N, d34S) of eel muscle tissues were able to differentiate among sample origins, with d34S values in particular discriminating among sites.

7. Recommendations

It is recommended that:

8.1 Elemental and stable isotopic patterns (d13C, d15N, d34S, $^{87}Sr/^{86}Sr$) of eel bodies together with metabolomic fingerprints need to be further explored for the geographic differentiation of glass eels.

8.2 Reference data specific to the year and estuary in question are likely to be required for any applied assignment

16. Acknowledgement

The authors thank the following people for helping with water and glass eel samples: Estibaliz Diaz and Maria Korta (AZTI), Brice Sauvaget and Cedric Briand (EPTB Vilaine) Peter Neusinger (Eeline UK Limited), Peter Wood (UK Glass Eels Limited), Ahmed Yahyaoui (Universite Mohammed) and Rachid Toujani (INSTM).

17. References

Beauchemin D, 2010. Inductively Coupled Plasma Mass Spectrometry. Analytical Chemistry **82**(12): 4786-4810.

Brigham RK and Jensen AC, 1964. Photographing Otoliths and Scales. The Progressive Fish-Culturist **26**(3): 131-135.

Brown RJ and Milton MJ, 2005. Analytical techniques for trace element analysis: an overview. TrAC Trends in Analytical Chemistry **24**(3): 266-274.

Bulska E and Ruszczyńska A, 2017. Analytical techniques for trace element determination. Physical Sciences Reviews **2**(5).

Donohoe C and Zimmerman C, 2010. A method of mounting multiple otoliths for beam-based microchemical analyses. Environmental Biology of Fishes **89**(3): 473-477.

Eriksson L, Trygg J, and Wold S, 2008. CV-ANOVA for significance testing of PLS and OPLS® models. Journal of Chemometrics **22**(11-12): 594-600.

EURACHEM. 2000. EURACHEM/CITAC Guide Quantifying Uncertainty in Analytical Measurement (2nd ed). Eurachem, London.

Evans D, Bartkevics V, Wickström H, 2014. Tracking stocked European eel (*Anguilla anguilla*) using otolith michrochemistry. Poster at ICES 5th International Otolith Symposium 20-24- October 2014.

Garcez RCS, Humston R, Harbor D, Freitas CES (2015) Otolith geo- chemistry in young-of-the-year peacock bass *Cichla temensis* for investigating natal dispersal in the Rio Negro (Amazon— Brazil) river system. Ecol Freshw Fish **24**:242–251

Horsky M, Irrgeher J, and Prohaska T, 2016. Evaluation strategies and uncertainty calculation of isotope amount ratios measured by MC ICP-MS on the example of Sr. Analytical and bioanalytical chemistry **408**(2): 351-367.

Irrgeher J, Prohaska T, Sturgeon RE, Mester Z, and Yang L, 2013. Determination of strontium isotope amount ratios in biological tissues using MC-ICPMS. Analytical Methods **5**(7): 1687-1694.

Irrgeher J, Vogl J, Santner J and Prohaska T, 2015. CHAPTER 8 Measurement Strategies. *In* Sector Field Mass Spectrometry for Elemental and Isotopic Analysis. The Royal Society of Chemistry. pp. 126-151.

Irrgeher J, Galler P and Prohaska T, 2016. 87Sr/86Sr isotope ratio measurements by laser ablation multicollector inductively coupled plasma mass spectrometry: Reconsidering matrix interferences in bioapatites and biogenic carbonates. Spectrochimica Acta Part B: Atomic Spectroscopy **125**: 31-42.

Kennedy BP, Folt CL, Blum JD, Chamberlain CP, 1997. Natural isotope markers in salmon. Nature (Lond.) **387**:766–767

Kennedy BP, Blum JD, Folt CL, Nislow KH, 2000. Using natural strontium isotopic signatures as fish markers: methodology and application. Can J Fish Aquat Sci **57**:2280–2292

Kennedy BP, Klaue A, Blum JD, Folt CL, Nislow KH, 2002. Reconstructing the lives of fish using Sr isotopes in otoliths. Can J Fish Aquat Sci **59**:925–929

Kiljunen M, Grey J, Sinisalo T, Harrod C, Immonen H, Jones RI, 2006. A revised model for lipid-normalizing d13C values from aquatic organisms, with implications ofr isotope mixing models. Journal of Applied Ecology **43**, 1213-1222

Krachler M, 2007. Environmental applications of single collector high resolution ICP-MS. Journal of Environmental Monitoring **9**(8): 790-804.

Marchante-Gayón JM 2004. Double-focusing ICP-MS for the analysis of biological materials. Analytical and Bioanalytical Chemistry **379**(3): 335-337.

Retzmann A, Zimmermann T, Pröfrock D, Prohaska T and Irrgeher J, 2017. A fully automated simultaneous single-stage separation of Sr, Pb, and Nd using DGA Resin for the isotopic analysis of marine sediments. Analytical and bioanalytical chemistry **409**(23): 5463-5480.

Zimmermann T, Retzmann A, Schober M, Pröfrock D, Prohaska T, and Irrgeher J, 2019. Matrix separation of Sr and Pb for isotopic ratio analysis of Ca-rich samples via an automated simultaneous separation procedure. Spectrochimica Acta Part B: Atomic Spectroscopy **151**: 54-64.

Zitek A, Irrgeher J, Cervicek M, Horsky M, Kletzl M, Weismann T, and Prohaska T, 2014. Individual-specific transgenerational marking of common carp *Cyprinus carpio*, L. using $^{86}Sr/^{84}Sr$ double spikes. Marine and Freshwater Research **65**(11): 978-986.